Biosynthesis of SiO_2 nanoparticles using extract of *Nerium oleander* leaves for the removal of tetracycline antibiotic

Noureddine El Messaoudi[a,*], Mohammed El Khomri[a], El-Houssaine Ablouh[b], Amal Bouich[c], Abdellah Lacherai[a], Amane Jada[d], Eder C. Lima[e], Farooq Sher[f,*]

[a]*Laboratory of Applied Chemistry and Environment, Ibn Zohr University, Agadir 80000, Morocco*

[b]*Materials Science, Energy and Nanoengineering Department (MSN), Mohammed VI Polytechnic University (UM6P), Benguerir 43150, Morocco*

[c]*Department of Applied Physics, Institute of Design and Manufacturing (IDF), Polytechnic University of Valencia, Valencia 46000, Spain*

[d]*Institute of Materials Science of Mulhouse (IS2M), High Alsace University, Mulhouse 68100, France*

[e] *Institute of Chemistry, The Federal University of Rio Grande do Sul (UFRGS), Porto Alegre-RS 91501-970, Brazil*

[f]*Department of Engineering, School of Science and Technology, Nottingham Trent University, Nottingham NG11 8NS, United Kingdom*

*Corresponding author:
Dr. F. Sher
Assistant Professor
Department of Engineering, School of Science and Technology
Nottingham Trent University
Nottingham
NG11 8NS
UK
E-mail address: Farooq.Sher@ntu.ac.uk
Tel.: +44 (0) 115 84 86679

Abstract

Tetracycline (TC) is one of the antibiotics that is found in wastewaters. TC is toxic, carcinogenic, and teratogenic. In this study, the tetracycline was removed from water by adsorption using dioxide silicon nanoparticles (SiO_2 NPs) biosynthesized from the extract of *Nerium oleander* leaves. These nanoparticles were characterized using SEM-EDX, BET-BJH, FTIR-ATR, TEM, and XRD. The influences of various factors such as pH solution, SiO_2 NPs dose, adsorption process time, initial TC concentration, and ionic strength on adsorption behaviour of TC onto SiO_2 NPs were investigated.TC adsorption on SiO_2 NPs could be well described in the pseudo-second-order kinetic model and followed the Langmuir isotherm model with a maximum adsorption capacity was 552.48 mg/g. At optimal conditions, the experimental adsorption results indicated that the SiO_2 NPs adsorbed 98.62% of TC. The removal of TC using SiO_2 NPs was 99.56% at conditions (SiO_2 NPs dose=0.25 g/L, C_0=25 mg/L, and t=40 min) based on Box–Behnken design (BBD) combined with response surface methodology (RSM) modelling. Electrostatic interaction governs the adsorption mechanism is attributed. The reusability of SiO_2 NPs was tested, and the performance adsorption was 85.36% after the five cycles. The synthesized SiO_2 NPs as promising adsorbent has a potential application for antibiotics removal from wastewaters.

Keywords: Green synthesis; Tetracycline; SiO_2 nanoparticles; *Nerium oleander* leaves extract; Chemical engineering; Adsorption and Optimization

1 Introduction

The excessive accumulation of toxic antibiotics in natural aquatic systems has received enormous attention due to their acute toxicity and possible carcinogenic effect (Grenni et al., 2018). Various antibiotics such as quinolones, sulfonamides, macrolides, and tetracyclines are broadly used to prevent and treat infectious diseases (Ahamad et al., 2019). Antibiotic residues, frequently found in soil, sediment, and aquatic environments, have adverse side effects as bacterial resistance changes in the microbial ecological functions (Sodhi et al., 2021). Antibiotic accumulation may also severely impair human physiological functions and have carcinogenic, teratogenic, or hormonal effects (Liu et al., 2017); their excess entrance into food chains may cause different disorders in the human body, such as the gastrointestinal system (Rashidi Nodeh et al., 2020). Therefore, controlling and handling antibiotic contaminants is necessary to have a safe environment (Yu et al., 2016).

Tetracycline (TC) is considered one of the most dangerous antibiotics due to its toxic, carcinogenic, and mutagenic effects (Scaria et al., 2021). TC is commonly used for animal husbandry and poultry industries worldwide to promote animal growth and prevent infections (Song et al., 2020; Van et al., 2020). About 60-80 % of tetracyclines were subject to different natural surroundings original in or metabolized forms due to lower metabolic rates in animals and humans (Epps and Blaney, 2016; Scaria et al., 2021); due to the high solubility rate, TC is detected in different water bodies and some regions; its concentration exceeds standard environmental limits (Daghrir and Drogui, 2013). Several approaches such as photocatalysis (Zhu et al., 2013), flocculation (Fu et al., 2015), biological treatment (Belkheiri et al., 2011), electrochemical (Wang et al., 2021), adsorption (Sharma et al., 2020), and reverse osmosis (Rostam and Taghizadeh, 2020) have been used to remove tetracycline from wastewaters. The adsorption process is a competitive and practical method for removing TC from wastewater due to high efficiency, low energy demand, and the possibility of reusing adsorbent materials (El Khomri et al., 2020; El Messaoudi et al., 2016a).

Consequently, a wide range of adsorbent materials (clays, chitosan, coated silica gel, zeolite ionic liquids, metal oxides, nanocomposites, nanomaterials, industrial and agricultural wastes) have already been tested for the recovery of TC contained in wastewater (Chang et al., 2012; Gao et al., 2012; Hao et al., 2021; Maged et al., 2020; Zhou et al., 2017). Recently, conducting nanoparticles such as ZrO_2 (Debnath et al., 2020), NiFe (Ravikumar et al., 2019), CeO_2 (Nurhasanah et al., 2020), La_2S_3 (Rashidi Nodeh et al., 2020), and ZnO (Bembibre et al., 2022) have been categorized as efficient adsorbents for TC removal from wastewaters due to high stability, porous nature, good adsorption aptitude, simple doping/dedoping, and ion exchange properties. Many methods have been used to synthesize the SiO_2 nanoparticles in the literature, such as solid-state, sonochemical (Masjedi-Arani et al., 2015), hydrothermal (Potapov et al., 2020), sol-gel (Dubey et al., 2015), and ultrasonic-assisted approaches (Ullah et al., 2019).

In this study, we used SiO_2 nanoparticles to remove TC from the aqueous solution because they are an excellent adsorbent to remove dyes and metals and a photocatalyst to treat wastewaters (Hosseini et al., 2018; Sharma et al., 2021). These nanoparticles are biosynthesized from the extract of *Nerium oleander* leaves. The biosynthesis of nanoparticles from the extract of agricultural solid wastes is regarded as a simple, rapid, cost-effective, and eco-friendly method for creating nanostructured materials such as metals, metal chalcogenides, and bimetal oxide (Das et al., 2018). In this work, we used the extract of *Nerium oleander* leaves for biosynthesized of SiO_2 nanoparticles. We chose this agricultural solid waste because its extract contains a significant amount of minerals, lost cost materials, and is eco-friendly and abundant in Morocco (Martín et al., 2018; Sebeia et al., 2019).

The performance of SiO_2 NPs was evaluated in this study by removing tetracycline from the solution aqueous. Besides, characterization techniques were practiced for investigating its structure and properties, such as scanning electron microscope coupled with energy-dispersive X-ray (SEM-EDX), Brunauer-Emmett-Teller and Barrett-Joyner-Halenda (BET-BJH), Fourier transform infrared spectroscopy coupled with attenuated total reflectance (FTIR-ATR), transition electron microscope (TEM), X-ray diffraction (XRD), and point of zero charge (PZC). The present work will substantially impact as it will add unique knowledge on the adsorption potential of SiO_2 NPs synthesized from the extract of *Nerium oleander* leaves. In this current study, the SiO_2 NPs were synthesized from the *Nerium oleander* leaves extract. Different influencing experimental parameters such as pH, SiO_2 NPs dose, reaction time, TC concentration, and ionic strength were investigated. Kinetic and equilibrium models evaluated the adsorption of TC on SiO_2 NPs. The removal of TC optimized using Box–Behnken design (BBD) combined with response surface methodology (RSM). The adsorption mechanism of TC molecules on the SiO_2 NPs surface was proposed. The reusability of SiO_2 NPs was evaluated.

2 Experimental

2.1 Materials

Nerium oleander leaves were collected in Tinghir (South-East Morocco). The silicate of sodium (Na_2SiO_3), tetracycline (antibiotic, $C_{22}H_{24}N_2O_8$, MW=444.435 g/mol), C_2H_5OH, HCl, and NaOH were parched from Sigma-Aldrich. The distilled and deionized waters were used through experiments.

2.2 Biosynthesis of SiO_2 NPs

10 g of *Nerium oleander* leave powder were added in 100 mL of C_2H_5OH and stirred for 3 h. After that, the solution was filtered using filter paper then the above mixture was centrifuged for obtained a clear extract of *Nerium oleander* leaves. 2 g Na_2SiO_3 and 50 mL of extract and 5 mL of NaOH (0.5 M) were mixed and stirred for 4 h (Dobrucka and Długaszewska, 2016). After precipitation, the mixture was filtered and centrifuged for separated the liquid and the precipitate (SiO_2 NPs). The residue obtained was watched with deionized water. Finally, The

SiO_2 nanoparticles were over-dried (80 °C) for 24 h and calcined in the furnace at 500 °C for 3 h (Shaligram et al., 2009).

2.3 Characterization

The physicochemical properties of SiO_2 NPs were examined using different characterization techniques. The morphology and microstructures of SiO_2 NPs were examined by SEM-EDX analysis (JEOL, JSM-IT200) and TEM analysis (Philips CM-30). BET and BJH methods (Belsorp Mini II) were used to determine the surface area, total pore volume, and diameter pore of SiO_2 NPs. The chemical bond characteristics of SiO_2 NPs before and after TC adsorption was acquired by FTIR-ATR analysis (Jasco 4100). The SiO_2 NPs crystal structures were evaluated using XRD analysis recorded on a 6100-Shimadzu. The PZC of adsorbent was determined using the method reported by Fiol and Villaescusa, (2009).

2.4 Batch adsorption experiments

The TC adsorption onto SiO_2 NPs nanoparticles was conducted in batch mode using 12.5 mg of SiO_2 NPs in 50 mL of TC solutions with concentrations varied from 50 to 200 mg/L at 23±1 °C. The influence of pH solution on adsorption was assessed and ranged from 3 to 11 and was adjusted by 0.01 M HCl acid or 0.01 M NaOH. The adsorbent dose, kinetic reaction, and ionic strength were changed from 0.05 to 0.4 g/L from 5 to 120 min and from 0 to 0.4 M, respectively. The separation of the solid-liquid phases was performed by centrifuging. The residual concentration was determined using a UV/Vis spectrophotometer (2300/Techcomp) at 376 nm as λ_{max} of TC. The quantity adsorbed q_e (mg/g) and the and TC removal efficiency (%) were obtained using following Eqs. (1) and (2) respectively (El Messaoudi et al., 2016b):

$$q_e = \frac{(C_0 - C_e) \times V}{w} \tag{1}$$

$$Percentage\ Removal\ (\%) = \frac{(C_0 - C_e)}{C_0} \times 100 \tag{2}$$

In equations (1) and (2), C_0 (mg/L) and C_e (mg/L) denote the concentrations of TC before and after adsorption, respectively. The w (g) and V (L) represents the weight of SiO_2 NPs and the volume of the reaction solution, respectively (Bentahar et al., 2018; El Messaoudi et al., 2017).

2.5 Experimental design

BBD used a static method to design experimental parameters influencing the adsorption of TC on SiO_2 NPs using design-expert software (version 12.0.3). TC concentration (A), reaction time (B), and SiO_2 NPs dose (C) as factors have significant effects on the TC adsorption on SiO_2 NPs at 23±1 °C and pH=5. Design of experiment runs and corresponding responses for TC removal efficiency by SiO_2 NPs are summarized in **Table 1**. A three-factors and levels (–1, 0, and 1) were applied to 21 experiments. The TC removal efficiency R (%) was expressed using the quadratic polynomial model was formalized in Eq. (3) (Jawad et al., 2020):

$$R(\%) = \sum_{I=1}^{3} \delta_i X_i + \sum_{I=1}^{3} \delta_{ii} X_i{}^2 + \sum_{I<j} \delta_{ij} X_i X_j + \delta_0 \qquad (3)$$

where δ_0 denotes constant-coefficient, δ_i is attributed to the direct effect, δ_{ii} corresponds to higher-order effect, and δ_{ij} denote reciprocate effect.

3 Results and discussion

3.1 Material characterization

The microstructures of synthesized nanoparticles were analyzed using SEM coupled with EDX. The results obtained are shown in **Fig. 1**. According to **Fig. 1(a)**, The SEM image of SiO_2 NPs showed that the particles are agglomerated and have poor dispersion. **Fig. 1(b)** represents the EDX spectrum and elemental analysis of SiO_2 NPs. The synthesis of SiO_2 NPs confirmed by the presence of O (53.82%) and Si (46.18%) (Dubey et al., 2015). **Fig. 1(c)** and **(d)** indicate the uniform distribution of O and Si was illustrated by EDX elemental mapping.

Fig. 2 illustrates the N_2 isotherms adsorption-desorption and average diameter distribution for SiO_2 NPs nanospheres. By means, BET and BJH methods, the obtained middle surface area, pore diameter, and total pore volume were 583.46 m^2/g, 3.46 nm, and 0.27 cm^3/g, respectively, confirmed the porosity of SiO_2 NPs. The FTIR spectra of SiO_2 NPs before and after the adsorption of TC (TC-SiO_2) are depicted in **Fig. 3**. On the spectrum of SiO_2 NPs, the broad bands at 3452 cm^{-1} and 1634 cm^{-1} correspond to OH stretching vibration and absorbed water molecule, respectively (El Messaoudi et al., 2016a; Niksefat et al., 2014).

The peaks at 1083 cm^{-1}, 953 cm^{-1} and 806 cm^{-1} and 457 cm^{-1} were ascribed to the Si-O stretching vibration, Si-OH stretching vibration and Si-O-Si symmetric stretching (Rafigh and Heydarinasab, 2017), and Si-O-Si bending, respectively (Yue et al., 2019), which confirms successful synthesis of SiO_2 nanospheres. The spectrum of TC-SiO_2 NPs shows small changes that demonstrate the TC adsorption on the surface of SiO_2 NPs. **Fig. 4(a)** shows the nanoparticles of SiO_2 NPs using a TEM image. According to this figure, the synthesized SiO_2 NPs particles were found to be spherical in structure (Dubey et al., 2015; Nita et al., 2019). The XRD characterization results of SiO_2 NPs are provided in **Fig. 4(b)**. A broad peak in the range of 20–30° is corresponded to the crystallite of SiO_2 particles (Rafigh and Heydarinasab, 2017), indicating the successful synthesis of SiO_2 NPs.

3.2 Adsorption study

3.2.1 Effect of solution pH

Fig. 5(a) presents the influence of pH on the TC adsorption at pH values ranging from 3 to11. This experiment attempted 10 mg of SiO_2 NPs in 50 mL of the solution TC (50 mg/L) at T=23 ±1 °C for 120 min. As **Fig. 5(a)** shows, the highest removal of TC was 98.07% at pH=5. Similar results were obtained by Debnath et al. (2020) and Rashidi Nodeh et al. (2020). This increase of TC removal in the acidic medium can be explained by the charge positive of SiO_2 NPs and the charge negative of TC (TCH^-, TC^-) (Li et al., 2010; Mohammed and Kareem, 2019). As **Fig. 10(a)** depicted, PZC of SiO_2 NPs was 8.2. The quantity adsorbed was 196.17

mg/g at pH=5. The dominance of charge positive of SiO_2 NPs at pH<PZC (adsorption of TC was favourable) and negatively charged when pH>PZC (adsorption of TC was unfavourable) (Song et al., 2020).

3.2.2 Effect of SiO_2 NPs dose

A TC concentration of 50 mg/L with a pH=5 at T=23 ±1 °C for 120 min, the effect of SiO_2 NPs dose (0.05-0.4 g/L) on TC adsorption was studied. **Fig. 5(b)** shows the results obtained. The TC removal increased from 54.38 to 98.92% by increasing the SiO_2 NPs dose from 0.05 to 0.25 g/L, while the quantity adsorbed decreased from 543.88 to 197.95 mg/g. Results imply that the number of active adsorption sites for TC adsorption corresponds to the applied dose, prompting higher removal efficiency (Zhang et al., 2019). After equilibrium between the adsorbent and antibiotic solution, the removal percentage remains consistent at higher dosages (> 0.25 g/L) (Jin et al., 2019). The optimum adsorbent dosage was considered 0.25 g/L to reach maximum TC removal efficiency, respectively.

3.2.3 Effect of contact time

The influence of the contact time on TC adsorption using SiO_2 NPs displayed in **Fig. 5(a)**. The contact time ranged from 5 to 120 min, whereas other parameters were kept constant (SiO_2 NPs=0.25 g/L, TC concentration=50 mg/L, pH=5, and T=23±1 °C). The TC adsorption was fast at first 30 min, which may be attributed to many sites accessible on the surface of the SiO_2 NPs in the initial phase (Ahamad et al., 2019). The equilibrium time was found to be 40 min. After equilibrium adsorption, the active sites were occupied by the TC molecule/ions. Therefore the adsorption rate became consistent (Zhou et al., 2020). Experimental data showed that stability was achieved in 40 min with an adsorption capacity of TC was 195.97 mg/g.

3.2.4 Effect of Initial TC concentration

The influence of TC concentration (25–200 mg/L) on its retention using SiO_2 NPs was studied with a fixed pH=5 and 0.25 g/L of SiO_2 NPs dose for 40 min. As illustrated in **Fig. 5(d)**, by increasing TC concentration from 25 to 150 mg/L, the TC adsorption capacity progressively increased from 99.40 to 512.06 mg/g, while the removal of TC decreased from 99.40 to 85.34%. This increases TC adsorption capacity due to the occupation of all available sites on the surface of SiO_2 nanoparticles by TC molecules (Debnath et al., 2020). After 150 mg/L, a plateau was not achieved in the adsorption capacity, suggesting active sites are still available and no saturation occurred. The phenomena were similar to the adsorption research of tetracycline reported previously (Ahamad et al., 2019; Ravikumar et al., 2019).

3.2.5 Effect of ionic strength

The electrolyte (NaCl) concentration in the aqueous solution significantly affects TC adsorption onto SiO_2 NPs. As reported in **Fig. 6**, at SiO_2 NPs=0.25 g/L, TC concentration=50 mg/L, pH=7, and T=23±1 °C, the removal efficiency of SiO_2 NPs for TC decreased from 73.15% (0 M NaCl) to 55.48% (0.4 M NaCl) by increasing the electrolyte concentrations from 0 to 0.4 M NaCl. By increasing the ionic strength, Cl^- competes with negatively charged TC (TCH^-, TC^-) species for adsorption onto SiO_2 NPs surface site with positively charged at pH=7 (Zhang et al., 2019). This result is in line with another study that reported a decline in TC adsorption onto clay surface sites, negatively charged by increasing electrolyte concentration in the solution (Parolo et al., 2008). In their study, by increasing Na^+ ion concentration at pH=4 of the solution, the competence for occupying surface sites between Na^+ ion and positively charged TC (TCH^+) increased (Yang et al., 2011). The reduction in TC adsorption onto the surface of clay increased in a higher concentration of Na^+ (Parolo et al., 2008).

3.3 Adsorption kinetics

The obtained experimental data were evaluated by using the pseudo-first-order (PFO) (Simonin, 2016), pseudo-second-order (PSO) (Ho and McKay, 1998), and intraparticle diffusion (IPD) (Graaf et al., 1990) kinetic models and their linear forms are given using the following Eqs. (4), (5), and (6) as represented in **Table 2**, respectively. **Table 2** also shows the parameters for linear fitting. Furthermore, the PSO model was fitted to data experimental based on R^2 (correlation coefficient). It can be found that R^2 values are very near to 1, and $q_{e,exp}$ values are also closer to $q_{e,cal}$ values for the PSO. This model speculates that adsorption pursues a second-order mechanism (El Messaoudi et al., 2021b).

3.4 Adsorption isotherm

The TC adsorption on SiO_2 NPs was the Langmuir (Langmuir, 1918), Freundlich (Freundlich, 1907), and Temkin (Johnson and Arnold, 1995) isotherm models. The linear forms of these isotherms are expressed on Eqs. (7), (8), and (9), as represented in **Table 3**. The parameters of linear fitting are listed in **Table 3**. Based on regression coefficients R^2 (0.9931, 0.9650, and 0.9392), the Langmuir model best described the TC adsorption on SiO_2 NPs. Langmuir model suggests the dye adsorption occurs as a monolayer from the homogeneous surface of the adsorbent (Bentahar et al., 2017; El Messaoudi et al., 2021a). A similar observation was found in other studies, showing successful adsorption isotherm data using Langmuir isotherm compared to Freundlich and Temkin isotherm models (Li et al., 2021; Mohammed et al., 2020). The maximum adsorption capacity *Qm* of SiO_2 NPs for TC adsorption was 552.48 mg/g. The comparison of the adsorption of SiO_2 NPs to remove TC from aqueous solution with other adsorbents reported in the literature is summarized in **Table 4**. Based on the results presented in this table, that the SiO_2 NPs exhibit high adsorption of TC compared with adsorbents. Therefore, SiO_2 NPs are a suitable adsorbent for the removal of antibiotic molecules from wastewater treatment.

3.5 Design optimization

Table 5 presents the results of ANOVA analysis of the statistical significance. The F-value (162.55) and p-value (<0.0001) indicate the polynomial equation was significant for the removal of TC on SiO_2 NPs within 95% (Hu et al., 2021). The high values of R^2 (0.9925), adjusted R^2 (0.9864), and predicted R^2 (0.9449) indicated the excellent fit of this model to the factors selected (Aziz et al., 2021). The value of adequate precision of 37.9356 (>4) shows a high level of statistical significance (Dalia Allouss et al., 2019). The predicated TC removal using SiO_2 NPs was obtained by the developed model represented below in Eq. (10) (Dalia Allouss et al., 2019).

$$R\,(\%) = 98.57 - 6.84\,A + 3.78\,B + 0.8861\,C + 3.72\,AB + 0.6362\,AC - 0.0713\,BC - 3.57A^2 - 2.36\,B^2 - 0.6527\,C^2 \quad (10)$$

The residual *vs*. predicted and 3D response surface plots of TC percentage are illustrated in **Fig. 7** and **Fig. 8**, respectively. The TC removal was experimentally 99.56% under optimal conditions (SiO_2 NPs dose=0.25 g/L, C_0=25 mg/L, and pH=5 at 23±1 °C for 40 min) RSM-BBD modeling.

3.6 Reusability of SiO_2 NPs

To assess the applicability of the adsorbent in the full-scale operation, the reusable capacity of SiO_2 NPs was studied for the removal of TC in optimal conditions (SiO_2 NPs dose=0.25 g/L, t=40 min, C_0=50 mg/L, pH (TC)=5, and T=23±1 °C). Therefore, the regeneration studies for evaluating the adsorption efficiency of the nanocomposite were conducted within five successive cycles using 0.1 M NaOH. According to **Fig. 9**, less than a 13% drop in the removal efficiency of TC occurred at the end of the fifth run, signifying the desirable reusability potential of the synthesized nanoparticles within successive runs of operation (Yang et al., 2020). This decrease was attributed to the occupation of available sites on the SiO_2 NPs surface (El Messaoudi et al., 2021b). In conclusion, the present adsorbent can be regarded as a promising material for practical application in environmental protection due to its excellent adsorption activities and high stability.

3.7 Proposed adsorption mechanism

Various mechanisms are involved in the adsorption of the organic compound to nanoparticle adsorbents. It was reported that both electrostatic and dispersive interaction between adsorbent and adsorbate is important in the adsorption process (Gao et al., 2019). Regarding the properties of organic adsorbate and adsorbent, the importance of each interaction is determined. As **Fig. 10(a)** shows, PZC of SiO_2 NPs was 8.2. The dominance of charge positive of SiO_2 NPs at pH<PZC and negatively charged when pH>PZC.The high value of PZC indicates the favourable and maximum adsorption in an acidic medium. This result confirmed the effect of pH on adsorption. The adsorption mechanism of TC on SiO_2 NPs is schematized in **Fig. 10(b)** based on PZC. The charge positive of SiO_2 NPs and the negative charge of TC indicates the governance of electrostatic interactions between TC and SiO_2 NPs (Gao et al., 2012).

4 Conclusions

The SiO_2 nanoparticles biosynthesized from the extract *Nerium oleander* leaves successfully with an effective method to remove tetracycline (TC) from an aqueous solution. The result of SEM-EDX, FTIR, TEM, and XRD characterization confirmed the biosynthesis of SiO_2 nanoparticles with spherical and crystallite in their structure. The parameters of the adsorption process were optimized with the variation in values of pH solution, SiO_2 NPs dose, adsorption process time, initial TC concentration, and ionic strength. Under conditions (SiO_2 NPs dose=0.25 g/L, t=40 min, C_0=50 mg/L, pH=5, and T=23±1 °C), the TC removal was 98.62%. The kinetics and isotherm of TC adsorption on SiO_2 NPs were described as the PSO and Langmuir models, respectively. The Qm was 552.48 mg/g. Optimization is an effective approach for modelling the sorption process of the TC on SiO_2 NPs using BBD–RSM. The recyclability study demonstrated that the SiO_2 NPs exhibited excellent reusability for TC removal. These results confirm that the SiO_2 NPs nanoparticles are suitable for removing antibiotics from wastewaters.

Acknowledgement

The authors are grateful for the financial supports from the Foundation for Research Support of the State of Rio Grande do Sul – FAPERGS [19/2551-0001865-7] and National Council for Scientific and Technological Development – CNPq [303.622/2017-2] and the Engineering and Physical Sciences Research Council (EPSRC) UK.

References

Ahamad, T., Ruksana, Chaudhary, A.A., Naushad, M., Alshehri, S.M., 2019. Fabrication of MnFe2O4 nanoparticles embedded chitosan-diphenylureaformaldehyde resin for the removal of tetracycline from aqueous solution. Int. J. Biol. Macromol. 134, 180–188. https://doi.org/10.1016/J.IJBIOMAC.2019.04.204

Aziz, K., Aziz, F., Mamouni, R., Aziz, L., Saffaj, N., 2021. Engineering of highly Brachychiton populneus shells@polyaniline bio-sorbent for efficient removal of pesticides from wastewater: Optimization using BBD-RSM approach. J. Mol. Liq. 117092. https://doi.org/10.1016/J.MOLLIQ.2021.117092

Belkheiri, D., Fourcade, F., Geneste, F., Floner, D., Aït-Amar, H., Amrane, A., 2011. Feasibility of an electrochemical pre-treatment prior to a biological treatment for tetracycline removal. Sep. Purif. Technol. 83, 151–156. https://doi.org/10.1016/J.SEPPUR.2011.09.029

Bembibre, A., Benamara, M., Hjiri, M., Gómez, E., Alamri, H.R., Dhahri, R., Serrà, A., 2022. Visible-light driven sonophotocatalytic removal of tetracycline using Ca-doped ZnO nanoparticles. Chem. Eng. J. 427, 132006. https://doi.org/10.1016/J.CEJ.2021.132006

Bentahar, S., Dbik, A., Khomri, M.E., El Messaoudi, N., Lacherai, A., 2018. Removal of a cationic dye from aqueous solution by natural clay. Groundw. Sustain. Dev. 6, 255–262. https://doi.org/10.1016/j.gsd.2018.02.002

Bentahar, S., Dbik, A., Khomri, M.E., El Messaoudi, N., Lacherai, A., 2017. Adsorption of methylene blue, crystal violet and congo red from binary and ternary systems with natural clay: Kinetic, isotherm, and thermodynamic. J. Environ. Chem. Eng. 5, 5921–5932. https://doi.org/10.1016/j.jece.2017.11.003

Chang, P.H., Li, Z., Jean, J.S., Jiang, W.T., Wang, C.J., Lin, K.H., 2012. Adsorption of tetracycline on 2:1 layered non-swelling clay mineral illite. Appl. Clay Sci. 67–68, 158–163. https://doi.org/10.1016/J.CLAY.2011.11.004

Daghrir, R., Drogui, P., 2013. Tetracycline antibiotics in the environment: a review. Environ. Chem. Lett. 2013 113 11, 209–227. https://doi.org/10.1007/S10311-013-0404-8

Dalia Allouss, Younes Essamlali, Othmane Amadine, Achraf Chakir, Mohamed Zahouily, 2019. Response surface methodology for optimization of methylene blue adsorption onto carboxymethyl cellulose-based hydrogel beads: adsorption kinetics, isotherm, thermodynamics and reusability studies. RSC Adv. 9, 37858–37869. https://doi.org/10.1039/C9RA06450H

Das, S., Chakraborty, J., Chatterjee, S., Kumar, H., 2018. Prospects of biosynthesized nanomaterials for the remediation of organic and inorganic environmental contaminants. Environ. Sci. Nano 5, 2784–2808. https://doi.org/10.1039/C8EN00799C

Debnath, B., Majumdar, M., Bhowmik, M., Bhowmik, K.L., Debnath, A., Roy, D.N., 2020. The effective adsorption of tetracycline onto zirconia nanoparticles synthesized by novel microbial green technology. J. Environ. Manage. 261, 110235. https://doi.org/10.1016/j.jenvman.2020.110235

Dobrucka, R., Długaszewska, J., 2016. Biosynthesis and antibacterial activity of ZnO nanoparticles using Trifolium pratense flower extract. Saudi J. Biol. Sci. 23, 517–523. https://doi.org/10.1016/J.SJBS.2015.05.016

Dubey, R.S., Rajesh, Y.B.R.D., More, M.A., 2015. Synthesis and Characterization of SiO2 Nanoparticles via Sol-gel Method for Industrial Applications. Mater. Today Proc. 2, 3575–3579. https://doi.org/10.1016/J.MATPR.2015.07.098

El Khomri, M., El Messaoudi, N., Dbik, A., Bentahar, S., Lacherai, A., 2020. Efficient adsorbent derived from Argania Spinosa for the adsorption of cationic dye: Kinetics,

mechanism, isotherm and thermodynamic study. Surfaces and Interfaces 20, 100601. https://doi.org/10.1016/j.surfin.2020.100601
El Messaoudi, N., Dbik, A., El Khomri, M., Sabour, A., Bentahar, S., Lacherai, A., 2017. Date stones of Phoenix dactylifera and jujube shells of Ziziphus lotus as potential biosorbents for anionic dye removal. Int. J. Phytoremediation 19, 1047–1052. https://doi.org/10.1080/15226514.2017.1319331
El Messaoudi, N., El Khomri, M., Bentahar, S., Dbik, A., Lacherai, A., Bakiz, B., 2016a. Evaluation of performance of chemically treated date stones: Application for the removal of cationic dyes from aqueous solutions. J. Taiwan Inst. Chem. Eng. 67, 244–253. https://doi.org/10.1016/j.jtice.2016.07.024
El Messaoudi, N., El Khomri, M., Chlif, N., Chegini, Z.G., Dbik, A., Bentahar, S., Lacherai, A., 2021a. Desorption of Congo red from dye-loaded Phoenix dactylifera date stones and Ziziphus lotus jujube shells. Groundw. Sustain. Dev. 12, 100552. https://doi.org/10.1016/j.gsd.2021.100552
El Messaoudi, N., El Khomri, M., Dabagh, A., Chegini, Z.G., Dbik, A., Bentahar, S., Lacherai, A., Iqbal, M., Jada, A., Sher, F., Lima, É.C., 2021b. Synthesis of a novel nanocomposite based on date stones/$CuFe_2O_4$ nanoparticles for eliminating cationic and anionic dyes from aqueous solution. Int. J. Environ. Stud. 1–19. https://doi.org/10.1080/00207233.2021.1929469
El Messaoudi, N., El Khomri, M., Dbik, A., Bentahar, S., Lacherai, A., Bakiz, B., 2016b. Biosorption of Congo red in a fixed-bed column from aqueous solution using jujube shell: Experimental and mathematical modeling. J. Environ. Chem. Eng. 4, 3848–3855. https://doi.org/10.1016/j.jece.2016.08.027
Epps, A. Van, Blaney, L., 2016. Antibiotic Residues in Animal Waste: Occurrence and Degradation in Conventional Agricultural Waste Management Practices. Curr. Pollut. Reports 2016 23 2, 135–155. https://doi.org/10.1007/S40726-016-0037-1
Fiol, N., Villaescusa, I., 2009. Determination of sorbent point zero charge: Usefulness in sorption studies. Environ. Chem. Lett. 7, 79–84. https://doi.org/10.1007/s10311-008-0139-0
Freundlich, H., 1907. Über die Adsorption in Lösungen. Zeitschrift für Phys. Chemie 57U, 385–470. https://doi.org/10.1515/ZPCH-1907-5723
Fu, Y., Peng, L., Zeng, Q., Yang, Y., Song, H., Shao, J., Liu, S., Gu, J., 2015. High efficient removal of tetracycline from solution by degradation and flocculation with nanoscale zerovalent iron. Chem. Eng. J. 270, 631–640. https://doi.org/10.1016/J.CEJ.2015.02.070
Gao, B., Li, P., Yang, R., Li, A., Yang, H., 2019. Investigation of multiple adsorption mechanisms for efficient removal of ofloxacin from water using lignin-based adsorbents. Sci. Reports 2019 91 9, 1–13. https://doi.org/10.1038/s41598-018-37206-1
Gao, Y., Li, Y., Zhang, L., Huang, H., Hu, J., Shah, S.M., Su, X., 2012. Adsorption and removal of tetracycline antibiotics from aqueous solution by graphene oxide. J. Colloid Interface Sci. 368, 540–546. https://doi.org/10.1016/J.JCIS.2011.11.015
Graaf, G.H., Scholtens, H., Stamhuis, E.J., Beenackers, A.A.C.M., 1990. Intra-particle diffusion limitations in low-pressure methanol synthesis. Chem. Eng. Sci. 45, 773–783. https://doi.org/10.1016/0009-2509(90)85001-T
Grenni, P., Ancona, V., Barra Caracciolo, A., 2018. Ecological effects of antibiotics on natural ecosystems: A review. Microchem. J. 136, 25–39. https://doi.org/10.1016/J.MICROC.2017.02.006
Hao, D., Chen, Y., Zhang, Y., You, N., 2021. Nanocomposites of zero-valent iron@biochar derived from agricultural wastes for adsorptive removal of tetracyclines. Chemosphere 284, 131342. https://doi.org/10.1016/J.CHEMOSPHERE.2021.131342
Ho, Y.S., McKay, G., 1998. Sorption of dye from aqueous solution by peat. Chem. Eng. J. 70,

115–124. https://doi.org/10.1016/S0923-0467(98)00076-1

Hosseini, S.A., Vossoughi, M., Mahmoodi, N.M., Sadrzadeh, M., 2018. Efficient dye removal from aqueous solution by high-performance electrospun nanofibrous membranes through incorporation of SiO2 nanoparticles. J. Clean. Prod. 183, 1197–1206. https://doi.org/10.1016/j.jclepro.2018.02.168

Hu, Y. ying, Pan, C., Zheng, X., Hu, F., Xu, L., Xu, G., Jian, Y., Peng, X., 2021. Prediction and optimization of adsorption properties for Cs+on NiSiO@NiAlFe LDHs hollow spheres from aqueous solution: Kinetics, isotherms, and BBD model. J. Hazard. Mater. 401, 123374. https://doi.org/10.1016/J.JHAZMAT.2020.123374

Jawad, A.H., Malek, N.N.A., Abdulhameed, A.S., Razuan, R., 2020. Synthesis of Magnetic Chitosan-Fly Ash/Fe3O4 Composite for Adsorption of Reactive Orange 16 Dye: Optimization by Box–Behnken Design. J. Polym. Environ. 28, 1068–1082. https://doi.org/10.1007/s10924-020-01669-z

Jin, J., Yang, Z., Xiong, W., Zhou, Y., Xu, R., Zhang, Y., Cao, J., Li, X., Zhou, C., 2019. Cu and Co nanoparticles co-doped MIL-101 as a novel adsorbent for efficient removal of tetracycline from aqueous solutions. Sci. Total Environ. 650, 408–418. https://doi.org/10.1016/J.SCITOTENV.2018.08.434

Johnson, R.D., Arnold, F.H., 1995. The temkin isotherm describes heterogeneous protein adsorption. Biochim. Biophys. Acta - Protein Struct. Mol. Enzymol. 1247, 293–297. https://doi.org/10.1016/0167-4838(95)00006-G

Langmuir, I., 1918. THE ADSORPTION OF GASES ON PLANE SURFACES OF GLASS, MICA AND PLATINUM. J. Am. Chem. Soc. 40, 1361–1403. https://doi.org/10.1021/JA02242A004

Li, S., Huang, W., Yang, P., Li, Z., Xia, B., Li, M., Xue, C., Liu, D., 2021. One-pot synthesis of N-doped carbon intercalated molybdenum disulfide nanohybrid for enhanced adsorption of tetracycline from aqueous solutions. Sci. Total Environ. 754, 141925. https://doi.org/10.1016/J.SCITOTENV.2020.141925

Li, Z., Schulz, L., Ackley, C., Fenske, N., 2010. Adsorption of tetracycline on kaolinite with pH-dependent surface charges. J. Colloid Interface Sci. 351, 254–260. https://doi.org/10.1016/J.JCIS.2010.07.034

Liu, F., Zhang, W., Chen, W., Wang, Jing, Yang, Q., Zhu, W., Wang, Jianlong, 2017. One-pot synthesis of NiFe2O4 integrated with EDTA-derived carbon dots for enhanced removal of tetracycline. Chem. Eng. J. 310, 187–196. https://doi.org/10.1016/J.CEJ.2016.10.116

Maged, A., Iqbal, J., Kharbish, S., Ismael, I.S., Bhatnagar, A., 2020. Tuning tetracycline removal from aqueous solution onto activated 2:1 layered clay mineral: Characterization, sorption and mechanistic studies. J. Hazard. Mater. 384, 121320. https://doi.org/10.1016/j.jhazmat.2019.121320

Martín, A., Caldelas, C., Weiss, D., Aranjuelo, I., Navarro, E., 2018. Assessment of Metal Immission in Urban Environments Using Elemental Concentrations and Zinc Isotope Signatures in Leaves of Nerium oleander. Environ. Sci. Technol. 52, 2071–2080. https://doi.org/10.1021/ACS.EST.7B00617

Masjedi-Arani, M., Ghanbari, D., Salavati-Niasari, M., Bagheri, S., 2015. Sonochemical Synthesis of Spherical Silica Nanoparticles and Polymeric Nanocomposites. J. Clust. Sci. 2015 271 27, 39–53. https://doi.org/10.1007/S10876-015-0897-3

Mohammed, A.A., Al-Musawi, T.J., Kareem, S.L., Zarrabi, M., Al-Ma'abreh, A.M., 2020. Simultaneous adsorption of tetracycline, amoxicillin, and ciprofloxacin by pistachio shell powder coated with zinc oxide nanoparticles. Arab. J. Chem. 13, 4629–4643. https://doi.org/10.1016/J.ARABJC.2019.10.010

Mohammed, A.A., Kareem, S.L., 2019. Adsorption of tetracycline fom wastewater by using Pistachio shell coated with ZnO nanoparticles: Equilibrium, kinetic and isotherm studies.

Alexandria Eng. J. 58, 917–928. https://doi.org/10.1016/J.AEJ.2019.08.006

Niksefat, N., Jahanshahi, M., Rahimpour, A., 2014. The effect of SiO2 nanoparticles on morphology and performance of thin film composite membranes for forward osmosis application. Desalination 343, 140–146. https://doi.org/10.1016/J.DESAL.2014.03.031

Nita, C., Fullenwarth, J., Monconduit, L., Le Meins, J.M., Fioux, P., Parmentier, J., Matei Ghimbeu, C., 2019. Eco-friendly synthesis of SiO2 nanoparticles confined in hard carbon: A promising material with unexpected mechanism for Li-ion batteries. Carbon N. Y. 143, 598–609. https://doi.org/10.1016/J.CARBON.2018.11.069

Nurhasanah, I., Kadarisman, Gunawan, V., Sutanto, H., 2020. Cerium oxide nanoparticles application for rapid adsorptive removal of tetracycline in water. J. Environ. Chem. Eng. 8, 103613. https://doi.org/10.1016/J.JECE.2019.103613

Parolo, M.E., Savini, M.C., Vallés, J.M., Baschini, M.T., Avena, M.J., 2008. Tetracycline adsorption on montmorillonite: pH and ionic strength effects. Appl. Clay Sci. 40, 179–186. https://doi.org/10.1016/J.CLAY.2007.08.003

Potapov, V., Fediuk, R., Gorev, D., 2020. Membrane concentration of hydrothermal SiO2 nanoparticles. Sep. Purif. Technol. 251, 117290. https://doi.org/10.1016/J.SEPPUR.2020.117290

Rafigh, S.M., Heydarinasab, A., 2017. Mesoporous Chitosan–SiO2 Nanoparticles: Synthesis, Characterization, and CO2 Adsorption Capacity. ACS Sustain. Chem. Eng. 5, 10379–10386. https://doi.org/10.1021/ACSSUSCHEMENG.7B02388

Rashidi Nodeh, H., Sereshti, H., Beirakabadi, E., Razmkhah, K., 2020. Synthesis and application of lanthanum sulfide nanoparticles for removal of tetracycline from aqueous media. Int. J. Environ. Sci. Technol. 17, 819–828. https://doi.org/10.1007/s13762-019-02399-z

Ravikumar, K.V.G., Sudakaran, S.V., Ravichandran, K., Pulimi, M., Natarajan, C., Mukherjee, A., 2019. Green synthesis of NiFe nano particles using Punica granatum peel extract for tetracycline removal. J. Clean. Prod. 210, 767–776. https://doi.org/10.1016/j.jclepro.2018.11.108

Rostam, A.B., Taghizadeh, M., 2020. Advanced oxidation processes integrated by membrane reactors and bioreactors for various wastewater treatments: A critical review. J. Environ. Chem. Eng. 8, 104566. https://doi.org/10.1016/J.JECE.2020.104566

Scaria, J., Anupama, K. V., Nidheesh, P. V., 2021. Tetracyclines in the environment: An overview on the occurrence, fate, toxicity, detection, removal methods, and sludge management. Sci. Total Environ. 771, 145291. https://doi.org/10.1016/J.SCITOTENV.2021.145291

Sebeia, N., Jabli, M., Ghith, A., 2019. Biological synthesis of copper nanoparticles, using Nerium oleander leaves extract: Characterization and study of their interaction with organic dyes. Inorg. Chem. Commun. 105, 36–46. https://doi.org/10.1016/J.INOCHE.2019.04.023

Shaligram, N.S., Bule, M., Bhambure, R., Singhal, R.S., Singh, S.K., Szakacs, G., Pandey, A., 2009. Biosynthesis of silver nanoparticles using aqueous extract from the compactin producing fungal strain. Process Biochem. 44, 939–943. https://doi.org/10.1016/J.PROCBIO.2009.04.009

Sharma, G., Bhogal, S., Kumar, A., Naushad, M., Sharma, S., Ahamad, T., Stadler, F.J., 2020. AgO/MgO/FeO@Si3N4 nanocomposite with robust adsorption capacity for tetracycline antibiotic removal from aqueous system. Adv. Powder Technol. 31, 4310–4318. https://doi.org/10.1016/J.APT.2020.09.006

Sharma, P., Kherb, J., Prakash, J., Kaushal, R., 2021. A novel and facile green synthesis of SiO2 nanoparticles for removal of toxic water pollutants. Appl. Nanosci. 2021 1–13. https://doi.org/10.1007/S13204-021-01898-1

Simonin, J.P., 2016. On the comparison of pseudo-first order and pseudo-second order rate laws in the modeling of adsorption kinetics. Chem. Eng. J. 300, 254–263. https://doi.org/10.1016/J.CEJ.2016.04.079

Sodhi, K.K., Kumar, M., Balan, B., Dhaulaniya, A.S., Shree, P., Sharma, N., Singh, D.K., 2021. Perspectives on the antibiotic contamination, resistance, metabolomics, and systemic remediation. SN Appl. Sci. 2021 32 3, 1–25. https://doi.org/10.1007/S42452-020-04003-3

Song, Y.X., Chen, S., You, N., Fan, H.T., Sun, L.N., 2020. Nanocomposites of zero-valent Iron@Activated carbon derived from corn stalk for adsorptive removal of tetracycline antibiotics. Chemosphere 255, 126917. https://doi.org/10.1016/J.CHEMOSPHERE.2020.126917

Ullah, Z., Man, Z., Khan, A.S., Muhammad, N., Mahmood, H., Ben Ghanem, O., Ahmad, P., Hassan Shah, M.U., Mamoon-Ur-Rashid, Raheel, M., 2019. Extraction of valuable chemicals from sustainable rice husk waste using ultrasonic assisted ionic liquids technology. J. Clean. Prod. 220, 620–629. https://doi.org/10.1016/J.JCLEPRO.2019.02.041

Van, T.T.H., Yidana, Z., Smooker, P.M., Coloe, P.J., 2020. Antibiotic use in food animals worldwide, with a focus on Africa: Pluses and minuses. J. Glob. Antimicrob. Resist. 20, 170–177. https://doi.org/10.1016/J.JGAR.2019.07.031

Wang, X., Li, F., Hu, X., Hua, T., 2021. Electrochemical advanced oxidation processes coupled with membrane filtration for degrading antibiotic residues: A review on its potential applications, advances, and challenges. Sci. Total Environ. 784, 146912. https://doi.org/10.1016/J.SCITOTENV.2021.146912

Yang, G., Gao, Q., Yang, S., Yin, S., Cai, X., Yu, X., Zhang, S., Fang, Y., 2020. Strong adsorption of tetracycline hydrochloride on magnetic carbon-coated cobalt oxide nanoparticles. Chemosphere 239, 124831. https://doi.org/10.1016/j.chemosphere.2019.124831

Yang, S., Hu, J., Chen, C., Shao, D., Wang, X., 2011. Mutual Effects of Pb(II) and Humic Acid Adsorption on Multiwalled Carbon Nanotubes/Polyacrylamide Composites from Aqueous Solutions. Environ. Sci. Technol. 45, 3621–3627. https://doi.org/10.1021/ES104047D

Yu, F., Li, Y., Han, S., Ma, J., 2016. Adsorptive removal of antibiotics from aqueous solution using carbon materials. Chemosphere 153, 365–385. https://doi.org/10.1016/J.CHEMOSPHERE.2016.03.083

Yue, Y., Peng, Z., Wang, W., Cai, Y., Tan, F., Wang, X., Qiao, X., 2019. Facile preparation of MgO-loaded SiO2 nanocomposites for tetracycline removal from aqueous solution. Powder Technol. 347, 1–9. https://doi.org/10.1016/J.POWTEC.2019.02.034

Zhang, X., Lin, X., He, Y., Chen, Y., Luo, X., Shang, R., 2019. Study on adsorption of tetracycline by Cu-immobilized alginate adsorbent from water environment. Int. J. Biol. Macromol. 124, 418–428. https://doi.org/10.1016/J.IJBIOMAC.2018.11.218

Zhou, J., Ma, F., Guo, H., 2020. Adsorption behavior of tetracycline from aqueous solution on ferroferric oxide nanoparticles assisted powdered activated carbon. Chem. Eng. J. 384, 123290. https://doi.org/10.1016/J.CEJ.2019.123290

Zhou, Y., Liu, X., Xiang, Y., Wang, P., Zhang, J., Zhang, F., Wei, J., Luo, L., Lei, M., Tang, L., 2017. Modification of biochar derived from sawdust and its application in removal of tetracycline and copper from aqueous solution: Adsorption mechanism and modelling. Bioresour. Technol. 245, 266–273. https://doi.org/10.1016/J.BIORTECH.2017.08.178

Zhu, X.D., Wang, Y.J., Sun, R.J., Zhou, D.M., 2013. Photocatalytic degradation of tetracycline in aqueous solution by nanosized TiO2. Chemosphere 92, 925–932. https://doi.org/10.1016/J.CHEMOSPHERE.2013.02.066

List of Figures

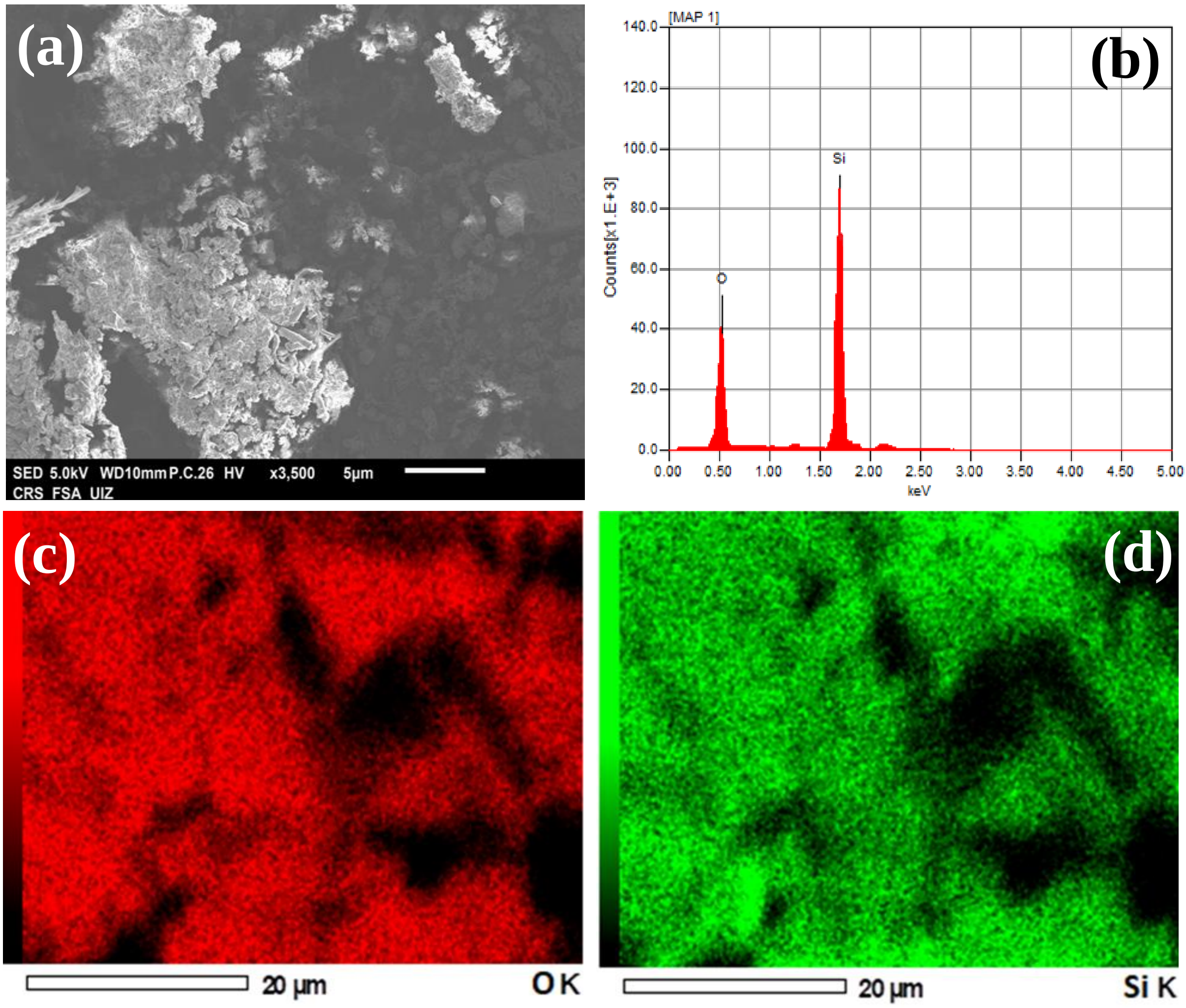

Fig. 1. SEM image; (**a**) SiO_2 NPs, (**b**) Elemental analysis, (**c**) Mapping image of SiO_2 NPs: oxygen and (**d**) Mapping image of silicon.

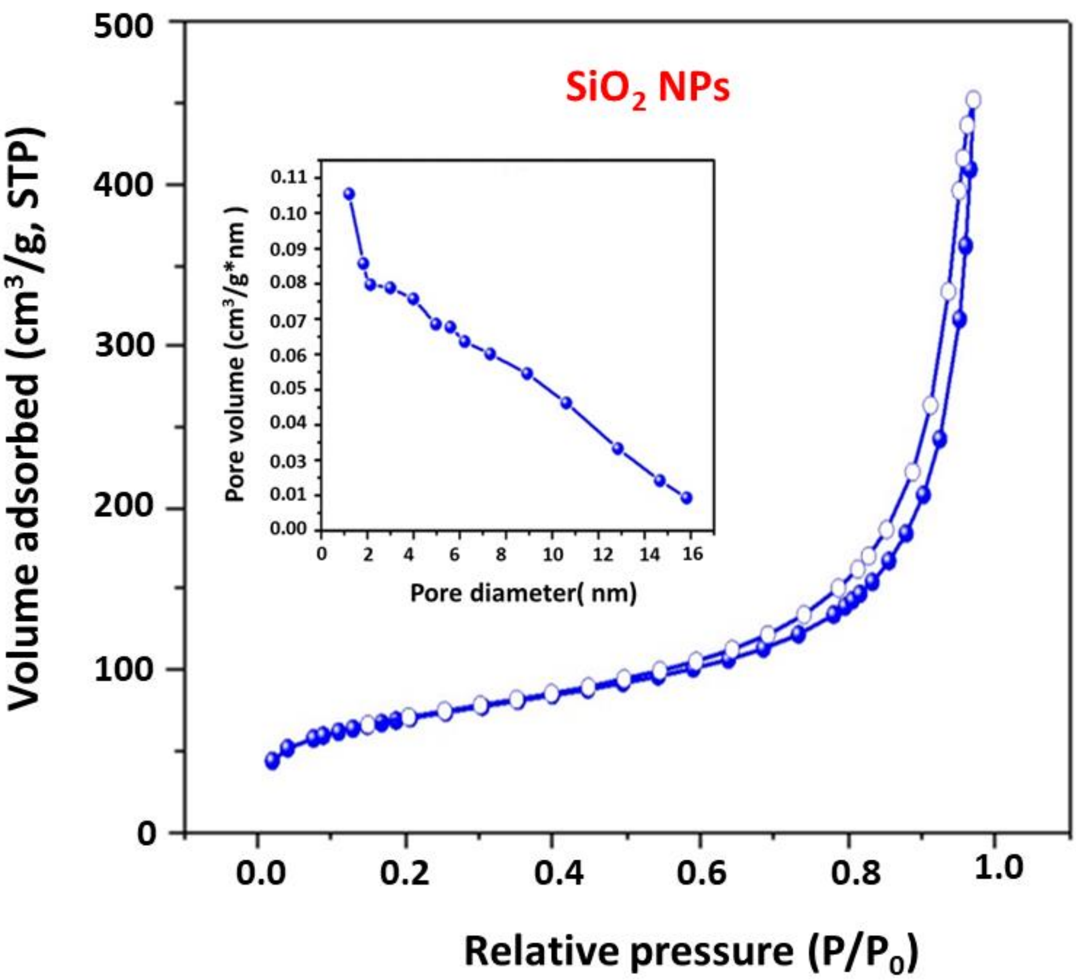

Fig. 2. N_2 adsorption/desorption isotherm curve and pore size distribution of TC-SiO_2 NPs.

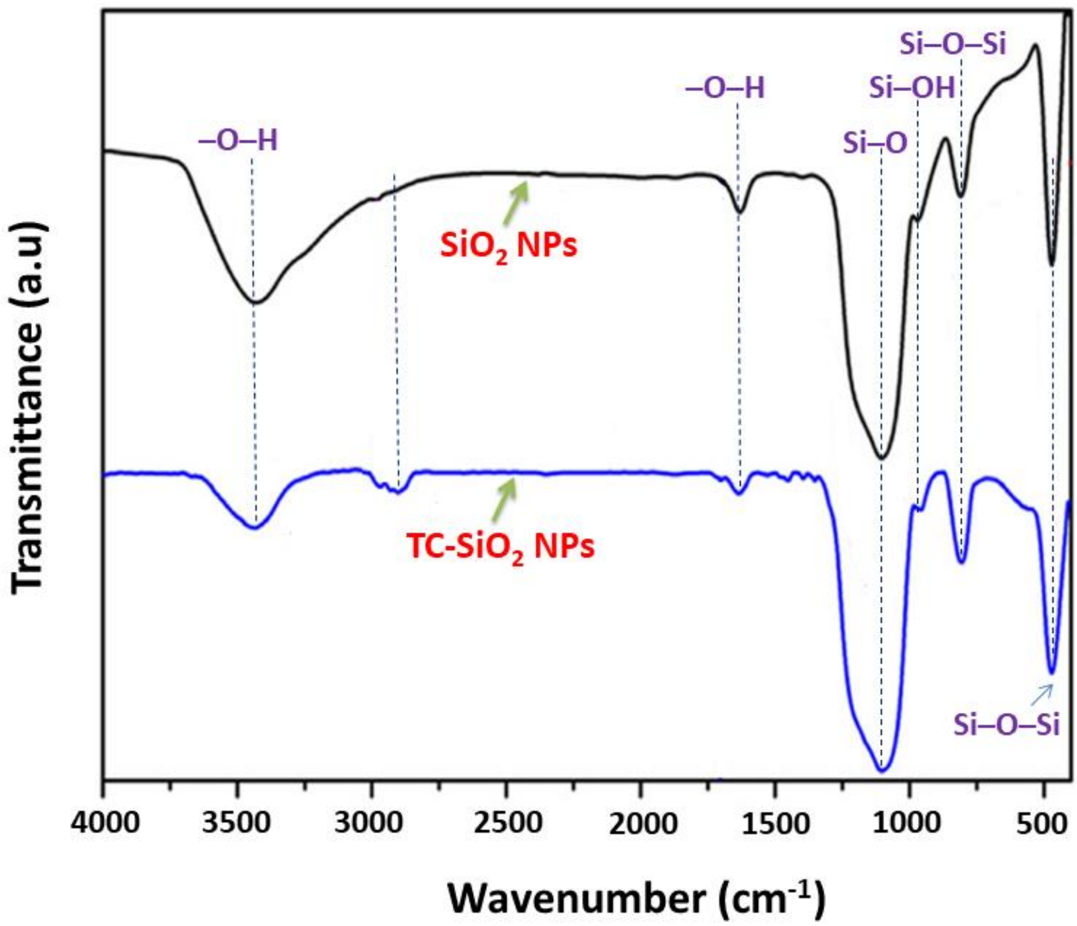

Fig. 3. FTIR spectra of SiO_2 NPs and TC-SiO_2 NPs (after adsorption).

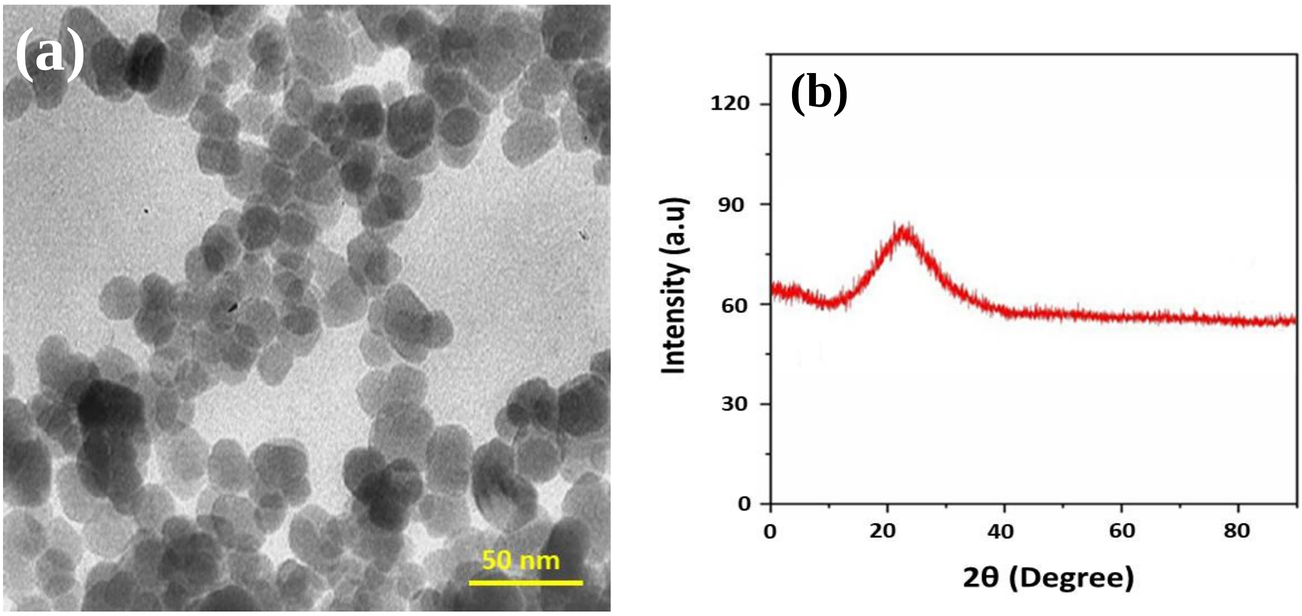

Fig. 4. SiO_2 NPs (**a**) TEM image and (**b**) XRD spectrum.

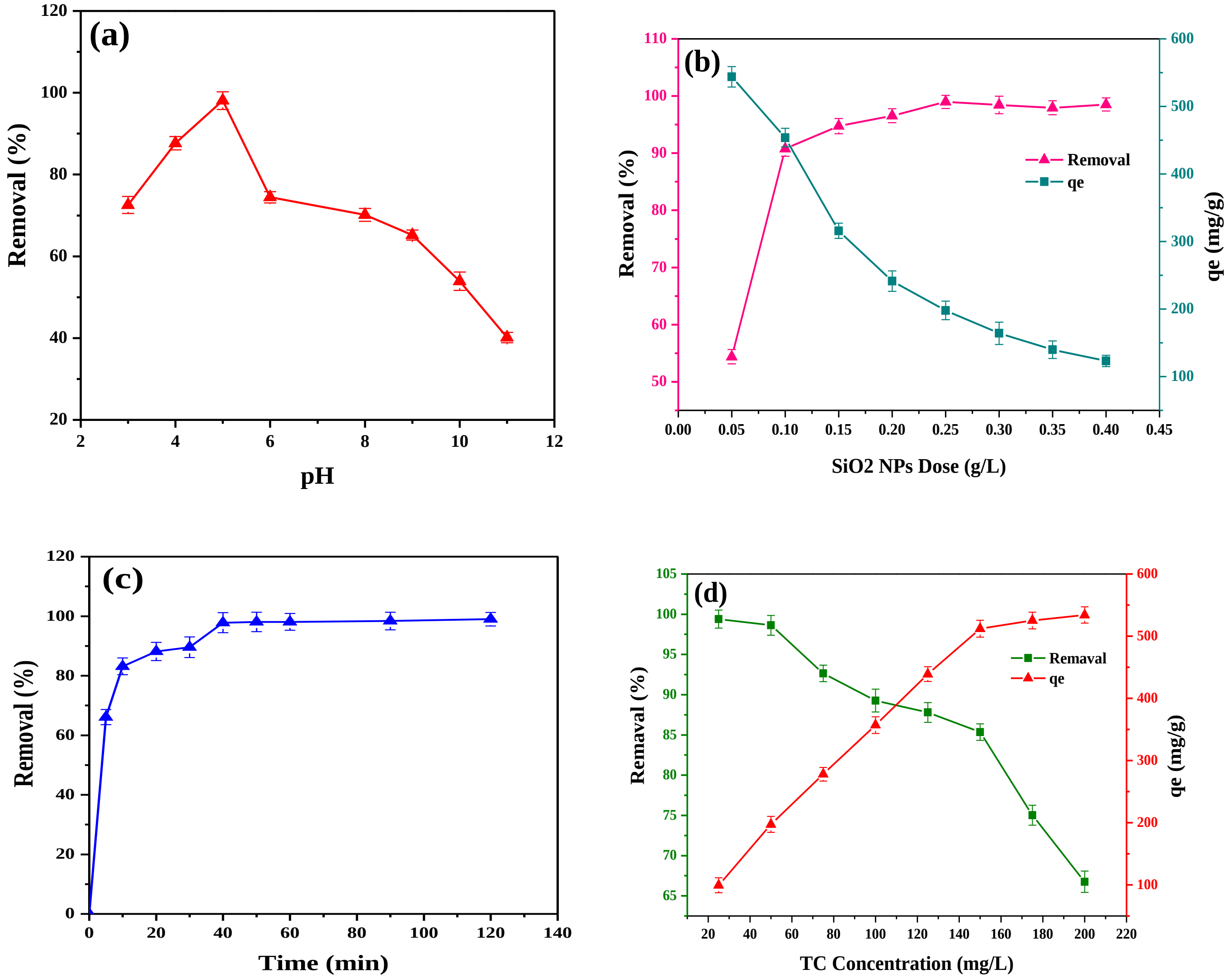

Fig. 5. Removal percentage using SiO_2 NPs; (**a**) Effects of pH, (**b**) Effect of SiO_2 NPs dose, (**c**) Effect of reaction time and (**d**) Effect of initial concentration on TC adsorption.

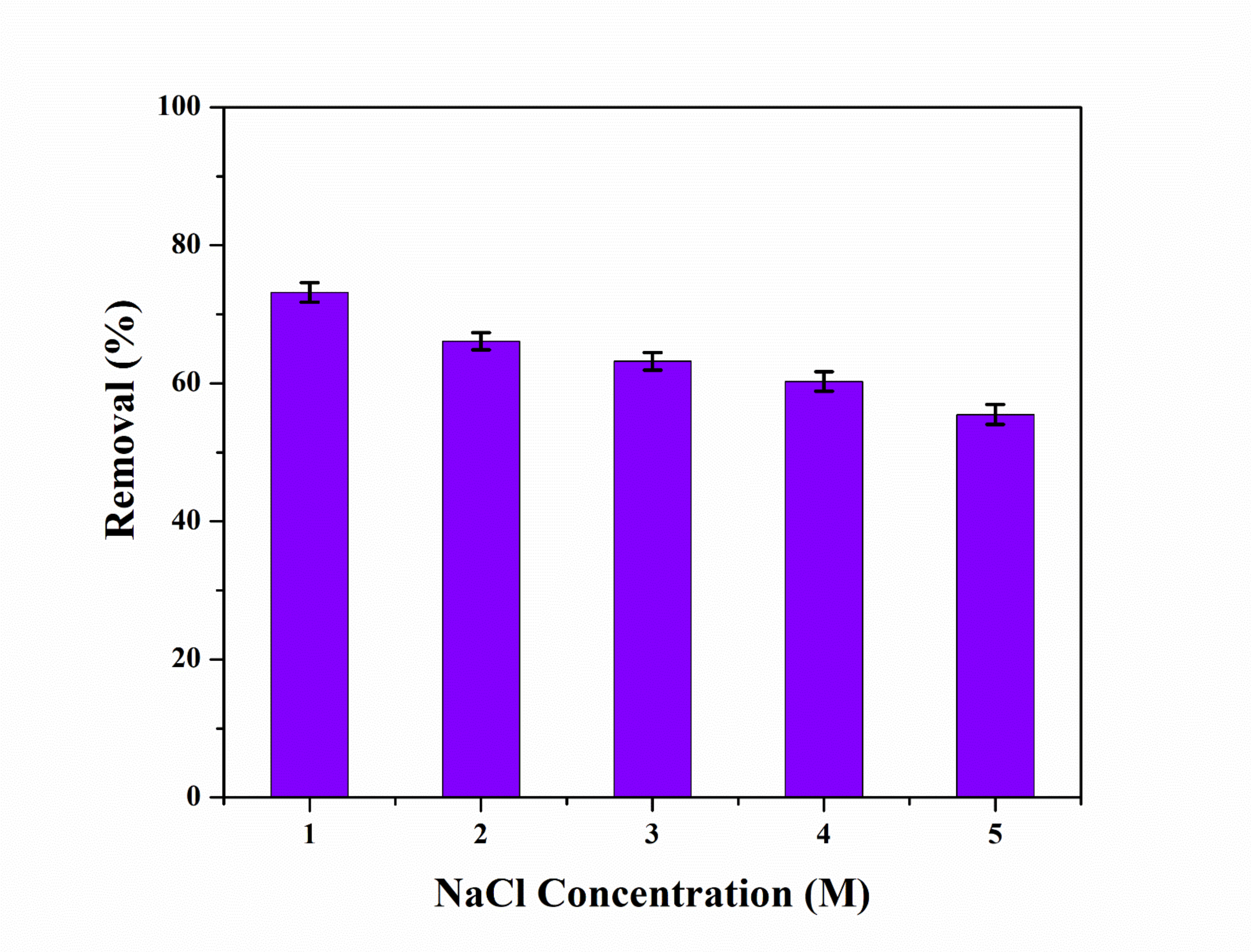

Fig. 6. Effect of ionic strength on TC adsorption using SiO_2 NPs.

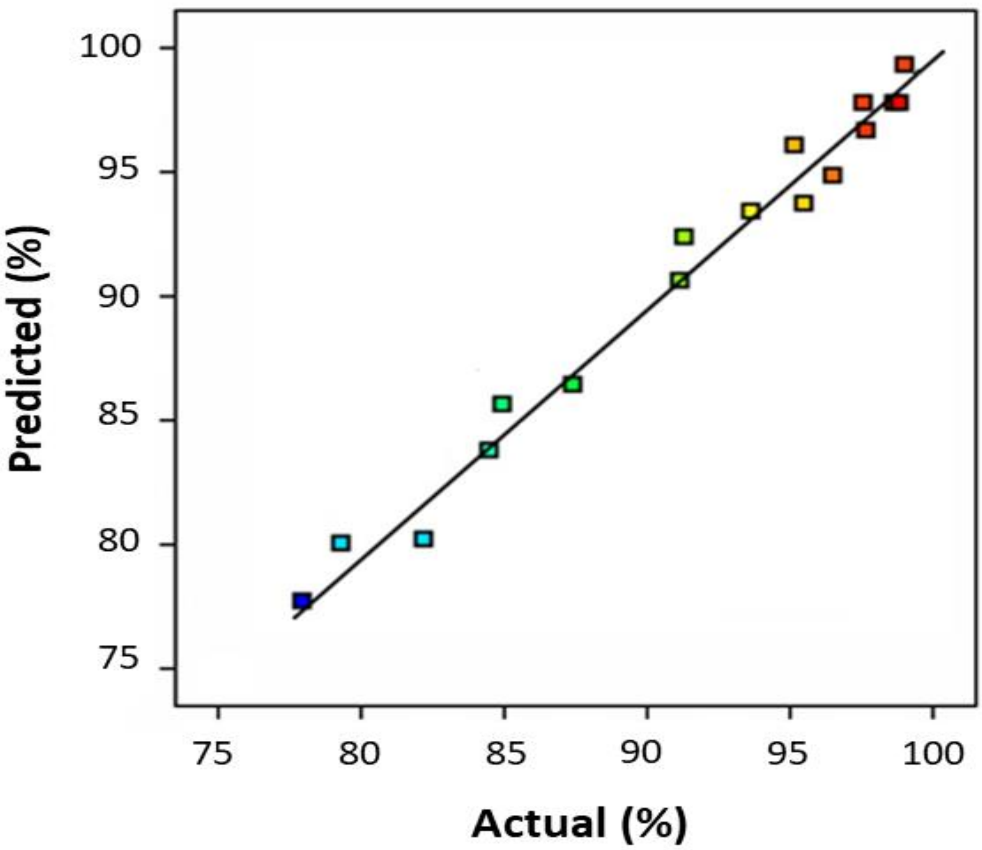

Fig. 7. Actual versus predicted for TC adsorption on SiO_2 NPs.

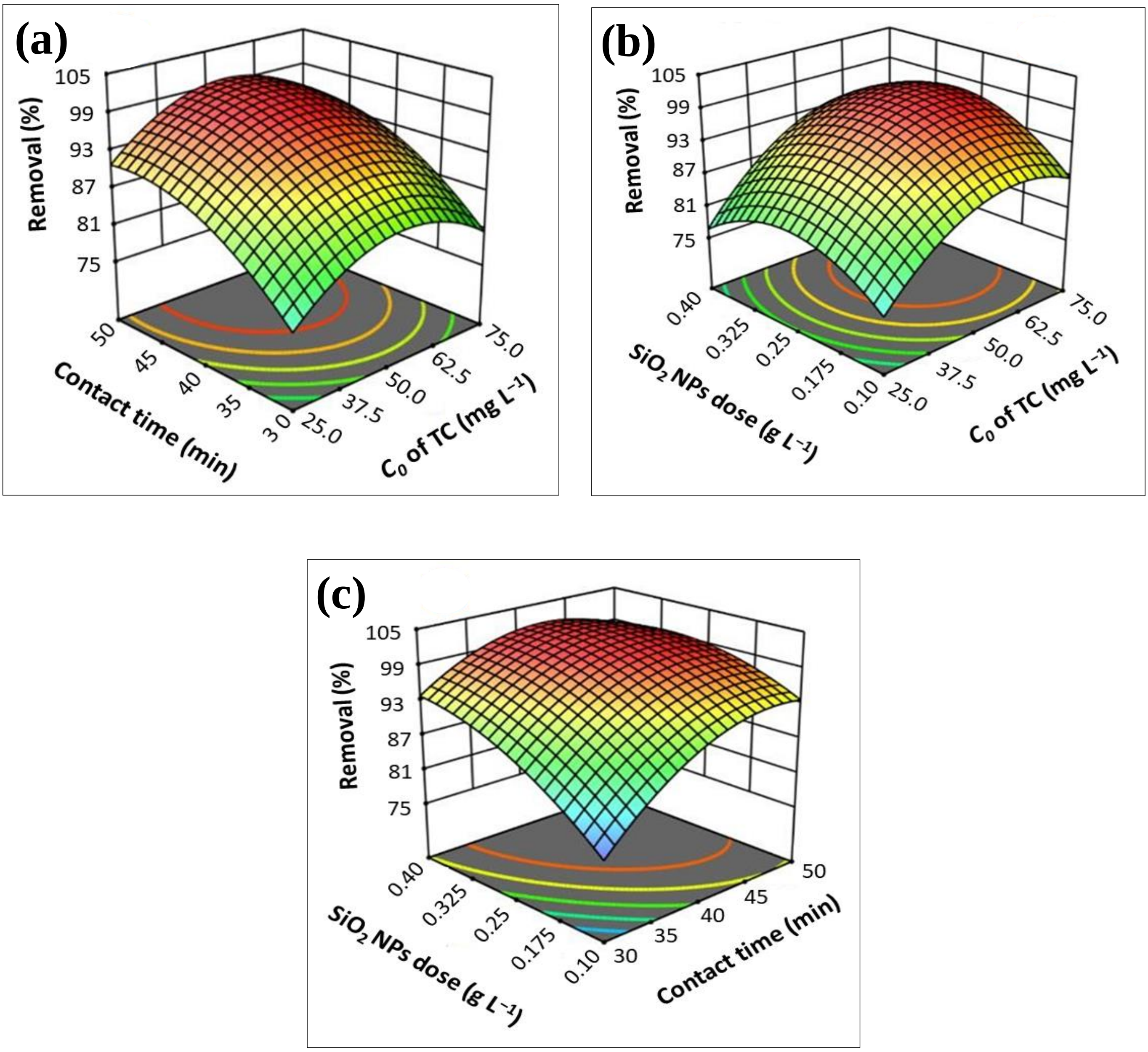

Fig. 8. Surface response plots of TC removal percentage; (**a**) Initial TC concentration with contact time, (**b**) SiO_2 NPs dose with initial TC concentration and (**c**) SiO_2 NPs dose with contact time.

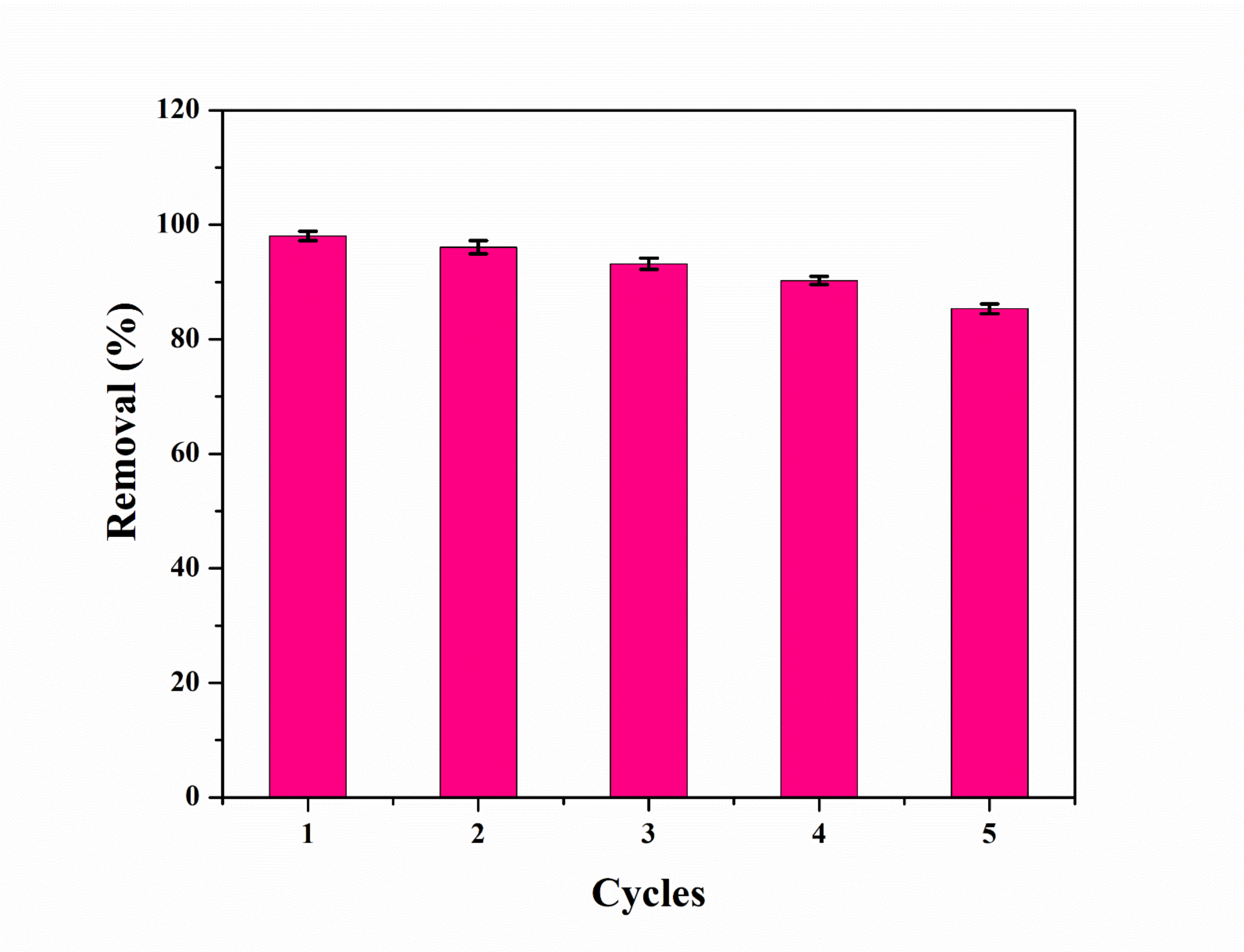

Fig.9. Reusability of SiO_2 NPs for the removal of TC.

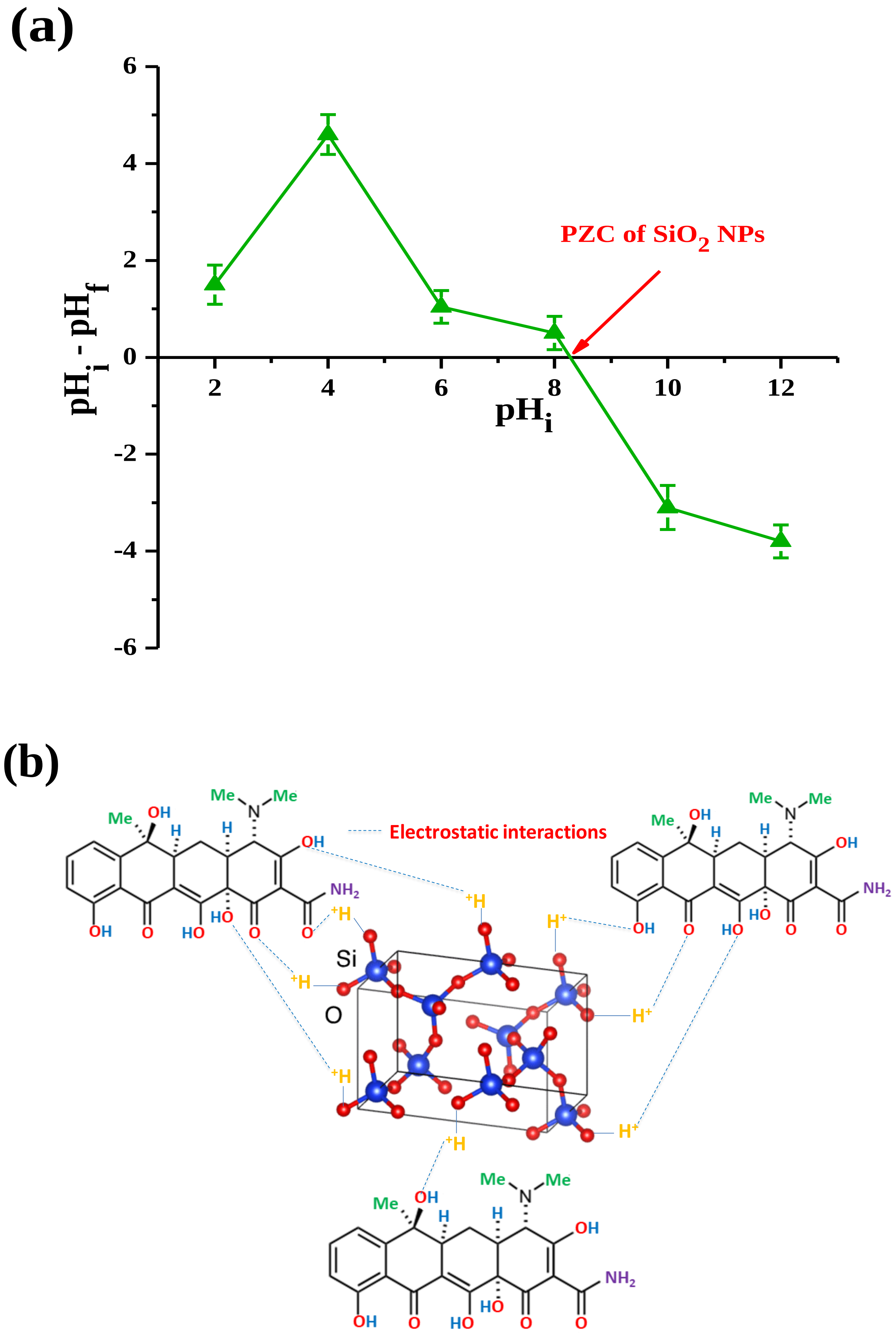

Fig. 10. (**a**) PZC of SiO_2 NPs and (**b**) Proposed adsorption mechanism of TC on SiO_2 NPs.

List of Tables

Table 1. Design of experiment runs and corresponding responses for TC removal efficiency by SiO_2 NPs.

Variables	**Codes**		
	-1	0	1
A=TC concentration (mg/L)	25	50	75
B=Contact time (min)	30	40	50
C=SiO_2 NPs dose (g/L)	0.1	0.25	0.4

Run	**A (mg/L)**	**B (min)**	**C (g/L)**	**R (%)**
1	25	30	0.1	98.05
2	75	30	0.1	77.11
3	25	50	0.1	98.87
4	75	50	0.1	90.11
5	25	30	0.4	99.23
6	75	30	0.4	78.13
7	25	50	0.4	99.06
8	75	50	0.4	93.55
9	25	40	0.25	99.56
10	75	40	0.25	90.57
11	50	30	0.25	89.45
12	50	50	0.25	98.66
13	50	40	0.1	90.11
14	50	40	0.4	98.65
15	50	40	0.25	98.44
16	50	40	0.25	98.71
17	50	40	0.25	98.24
18	50	40	0.25	98.53
19	50	40	0.25	98.61
20	50	40	0.25	98.72
21	50	40	0.25	98.23

Table 2. Kinetic model parameters for the TC adsorption ontoSiO_2 NPs.

Model and its equation		**Parameter**	**Value**
		$q_{e,exp}$ (mg/g)	197.98
PFO		$q_{e,cal}$ (mg/g)	51.03
$Log(q_e - q_t) = Log(q_e) - \frac{K_{PFO}}{2.303}t$ (4)		K_{PFO} (1/min)	0.0052
		R^2	0.8285
PSO		$q_{e,cal}$ (mg/g)	204.08
$\frac{t}{q_t} = \frac{1}{K_{PSO}{q_e}^2} + \frac{1}{q_e}t$ (5)		K_{PSO} (g/mg.min)	0.0019
		R^2	0.9996
		K_{IPD1} (mg/g.min$^{1/2}$)	16.0461
	1st linear portion	C_1 (mg/g)	35.28
		R^2	0.9811
		K_{IPD2} (mg/g.min$^{1/2}$)	10.1487
IPD	2nd linear portion	C_2 (mg/g)	49.76
$q_t = K_{IPD}t^{1/2} + C$ (6)		R^2	0.9045
		K_{IPD3} (mg/g.min$^{1/2}$)	3.1460
	3rd linear portion	C_3 (mg/g)	62.75
		R^2	0.9733

Notation: K_{PFO} (1/min)=PFO rate constant, K_{PSO} (g/mg/min)=PSO rate constant, K_{IPD} (mg/g.min$^{1/2}$)=IPD rate constant, C(mg/g)=Constant for any experiment, q_t (mg/g)=Amount adsorbed of TC at time t, and q_e (mg/g)=Amount adsorbed of TC at equilibrium (Graaf et al., 1990; Ho and McKay, 1998; Simonin, 2016)

Table 3. Isotherm model parameters for the TC adsorption onto SiO_2 NPs.

Model and its equation		Parameter	Value
Langmuir		Q_m (mg/g)	552.48
$\frac{C_e}{q_e} = \frac{1}{Q_m K_L} + \frac{C_e}{Q_m}$	(7)	K_L (L/mg)	0.3175
		R^2	0.9931
Freundlich		K_F (mg/g)	188.7644
$Lnq_e = LnK_F + \frac{LnC_e}{n}$	(8)	N	03.5997
		R^2	0.9650
Temkin		K_T (L/g)	18.3610
$q_e = BLnK_T + BLnC_e$	(9)	B	75.6710
		R^2	0.9392

Notation: C_e (mg/L)=Equilibrium concentration of TC, Q_m (mg/g)=Monolayer (maximum) adsorption capacity, K_L (L/mg)=Langmuir rate constant, K_F (mg/g)=Freundlich rate constant, n=Heterogeneity factor, K_T (L/g)=Temkin rate constant, and B=constant related to the heat adsorption (Freundlich, 1907; Johnson and Arnold, 1995; Langmuir, 1918)

Table 4. Comparison of the adsorption of SiO_2 NPs for TC with other adsorbents reported in the literature.

Adsorbent	**Ad (mg/L)**	**T (°C)**	***t* (min)**	**C_0 (mg/L)**	**pH**	**Q_m (mg/g)**	**Reference**
ZrO_2 NPs	0.2	–	15	25–150	6	526.32	(Debnath et al., 2020)
AgO/MgO/FeO@Si_3N_4	–	30	90	30–100	8	172.41	(Sharma et al., 2020)
ACCS	02.5	–	20	100–700	5	38.30	(Song et al., 2020)
ZVI@ACCS	02.5	–	20	100–700	5	78.30	(Song et al., 2020)
NiFe2O4@CDs	10	50	1440	25–100	8	591.72	(Liu et al., 2017)
Pristine MoS_2	0.4	35	2400	50–500	6	409.84	(Li et al., 2021)
NiFe NPs	0.3	–	90	20–80	7	61.00	(Ravikumar et al., 2019)
La_2S_3 NPs	1	25	90	10–300	5	56.81	(Rashidi Nodeh et al., 2020)
SiO_2 NPs	0.25	23	40	25–200	5	552.48	Current study

Notation : Ad=Adsobent dose, T=Temperature, t=Time, C_0= Initial TC concenration.

Table 5. ANOVA analysis and regression coefficients for the designed statistical model.

Source	**Sun Squares**	**Df**	**Mean Square**	**F-value**	**p-value**
Model	1221.20	9	135.69	162.55	< 0.0001
A-TC concentration	639.35	1	639.35	765.93	< 0.0001
B -Contact time	195.12	1	195.12	233.75	< 0.0001
C- SiO_2 NPs dose	10.72	1	10.72	12.85	0.0043
AB	110.78	1	110.78	132.71	< 0.0001
AC	03.24	1	03.24	03.88	0.0746
BC	0.0406	1	0.0406	0.0487	0.8295
A^2	191.81	1	191.81	229.78	< 0.0001
B^2	83.37	1	83.37	99.88	< 0.0001
C^2	06.39	1	06.39	07.66	0.0183
Residual	09.18	11	0.8347		
Lack of Fit	08.85	5	01.77	31.76	0.0003
Pure Error	0.3343	6	0.0557		
Core total	1230.38	20			
Model statistics	R^2	Adjusted R^2	Predicted R^2	Adequate precision	
	0.9925	0.9864	0.9449	37.9356	